# Impact & Energy Absorption of Road Safety Barriers by Coupled SPH /FEM

**I. Thiyahuddin[1], Y.T. Gu[1], D. P. Thambiratnam[2*], P. Gudimetla**
[1]School of Chemistry, Physics and Mechanical Engineering and [2]School of Civil Engineering and Built Environment
Queensland University of Technology, 4000 Brisbane, Australia
mohd.thiyahuddin@qut.edu.au, yuantong.gu@qut.edu.au,
*d.thambiratnam@qut.edu.au
*corresponding author
[Received date; Accepted date] – to be inserted later

**Abstract**
Road safety barriers are used to minimise the severity of road accidents and protect lives and property. There are several types of barrier in use today. This paper reports the initial phase of research carried out to study the impact response of portable water-filled barrier (PWFB) which has the potential to absorb impact energy and hence provide crash mitigation under low to moderate speeds. Current research on the impact and energy absorption capacity of water-filled road safety barriers is limited due to the complexity of fluid-structure interaction under dynamic impact. In this paper, a novel fluid-structure interaction method is developed based on the combination of Smooth Particle Hydrodynamics (SPH) and Finite Element Method (FEM). The sloshing phenomenon of water inside a PWFB is investigated to explore the energy absorption capacity of water under dynamic impact. It was found that water plays an important role in energy absorption. The coupling analysis developed in this paper will provide a platform to further the research in optimising the behaviour of the PWFB. The effect of the amount of water on its energy absorption capacity is investigated and the results have practical applications in the design of PWFBs.

## 1. INTRODUCTION

From 2000-2008, there has been 1500 accidents per year on Australian roads. Traffic accidents in Australia cost approximately $17.85 billion per year or 1.7% of the nation's GDP[1, 2]. These numbers includes the costs of road maintenance, emergency response units, road reconstruction crews and insurance claims [3]. Serious injuries sustained from accidents have long-term impacts with high medical costs, rehabilitation and permanent disabilities affecting the society.

Road safety barriers are roadside appurtenances that function to keep vehicles within their roadway and prevent errant vehicles from colliding with dangerous roadside obstacles or cause injuries to roadside workers. There are many types of road safety barriers being used in Australian roads today. Portable water filled barriers (PWFB) are in the semi-rigid group of roadside barriers. When filled with water, a road safety barrier has the potential to display good crash attenuation characteristics at low and moderate impact speeds[4]. The usage of water in a portable water-filled road barrier is mainly as anchorage for the barrier to remain stationary. However, the crash attenuation characteristic of water inside the barrier has not been extensively studied due to the complexities of the fluid-structure interaction. At the moment, there are no standards or recommended value to set how much water should be added inside PWFB. Existing water-filled road barriers relatively weigh at 70 kg when empty and can be filled up to 600 kg of water. Water has the potential to absorb some of the impact energy by transferring the kinetic energy from the impact to sloshing motion inside the barrier.

Several numerical studies and experiments [5-9] have been conducted to test their performance of these road barriers in the event of a roadside collision. However, as mentioned above, there is relatively little literature on studies of PWFBs. Ralph Grzebieta [5] conducted extensive full-scale impact tests of a variety road barriers [5, 8] and provided some recommendations to make Australian roads safer. Ulker [7] conducted experiments on concrete barriers along with Finite

Element Analysis (FEA) in his research. Ren [9] conducted numerical simulations of steel barriers impacted by a small-sedan car. Subsequently, Borovins [6] simulated the impact of large vehicle onto steel barriers. Though steel barriers may perform well under impact with a normal car, Borovins research investigated whether they could perform well under impacts with larger vehicles such as trucks and buses. Although Ren [9] and Borovins [6] did not suggest a definitive argument in containment by redirecting the vehicle and the deflection of the steel barrier; they suggested that Finite Element Method (FEM) to be the best method for initial evaluation before proceeding to full scale field experiments

A large amount of studies on fluid sloshing have been carried out using the Eulerian and Augmented Lagrange & Eulerian (ALE) methods [10-16] due to their ability to replicate sloshing accurately. The application of ALE has been widely used in sloshing problems involving free surfaces and high velocity impact problems [17, 18]. In both methods, the air inside the barrier will also need to be modeled, requiring higher computation time without increased accuracy in results [17]. Housner's [19] pioneering work in fluid dynamics was extended to other areas such as dam-water interaction under earthquakes, collisions between ships, and anything else that involved sloshing of fluids.[18, 20-27].

The Smoothed Particle Hydrodynamics (SPH) method has been developed to model fluid regions in several applications [17, 28]. SPH is able to do this well, but it requires high computational resources[17]. Although the accuracy and precision of FEM method is at its peak with the advent of supercomputers and improved computational power, the method is limited to gridded element mesh and is unable to produce efficient result in problems related to high fluid motions such as in high velocity-impacts and explosions [17, 28-31]. These types of motion are evident for fluid in PWFBs.

The numerical modelling of road safety barriers will need to deal with high velocity impact problems involving multiple bodies, large deformations and complex fluid-structure interaction. The traditional numerical FEM alone fails to handle this problem with precision. On the other hand, the use of SPH in all parts of the model will require significant amount of computational power. Moreover, the use of finite elements in the solid domain of the barrier increases the accuracy of the structural analysis [32]. Therefore, a coupled analysis technique incorporating both FEA and SPH can be used to model the PWFB to achieve the required results efficiently without exhausting the computational resources. This type of analysis has not been extensively performed where there is high rates of deformation of the fluid due to the impact.

This paper presents the initial research carried out to simulate the impact response and energy absorption of a PWFB. It involves the response of a water filled container under the impact of a rigid block. A coupled analysis combining SPH with FEM is developed and used in this study. The sloshing phenomenon of water inside the shell container under impact is investigated using the software package LSTC-DYNA 971. The effects of the amounts of water on the sloshing response and hence the ability to absorb impact energy are investigated. The results provide interesting and important information that will be directly applicable to the design of a proto-type PWFBs.

## 2. THE SPH METHOD FOR FLUID SIMULATION

### 2.1 SMOOTHED PARTICLE HYDRODYNAMICS (SPH)

SPH is a meshless computational Lagrangian hydrodynamic particle method. This method originated approximately 30 years ago when it was [33, 34] used to model astrophysical phenomena without boundaries. This method of modelling makes use of particles as the frame for computational interpolation and as carrier of material properties. It has been used in many fields of research including astrophysics, ballistics, vulcanology, solid mechanics and oceanography. The resolution of the method can easily be adjusted with respect to variables such as the density [35].

The SPH system is represented by a finite number of particles that carry individual mass and occupy individual space. SPH is based on interpolation theory by utilising kernel approximation and particles approximation respectively. The conservation laws of continuum dynamics in the form of partial differential equations are transformed into integral equations through the use of an interpolation function for kernel estimation. The main features of SPH were extensively described by Liu [29, 30], Monaghan [36] and Benz [37] and will only be referred below by the

representation of the constitutive equation in SPH notations. The kernel approximation can be illustrated by the following identity on eqn. (1):

$$f(x) = \int_{\Omega} f(\vec{x}')W(\vec{x} - \vec{x}', h)d\vec{x}' \tag{1}$$

with $W(\vec{x} - \vec{x}', h)$ as the smoothing function. The function $W$ is usually chosen to be an even function that satisfies the normalization condition, delta function property and the compact condition which are outlined in eqns. (2-4).

*Normalization condition*

$$\int_{\Omega} W(\vec{x} - \vec{x}', h) = 1 \tag{2}$$

*Delta function property condition*

$$\lim_{h \to 0} W(\vec{x} - \vec{x}', h) = d(x - x') \tag{3}$$

*Compact condition*

$$W(\vec{x} - \vec{x}', h) = 0 \; when \; |x - x'| > \kappa h; \tag{4}$$

$\kappa$ is a constant to the smoothing function, the kernel approximation consists of integration of the multiplication of an arbitrary function and smoothing kernel function. The integral represent an approximation by summing up values of all the neighbouring particles. Particle approximation provides the necessary stability to the SPH method. The approximation leads to eqn. (5):

$$< f(x_i) >= \sum_{j=1} \frac{m_j}{\rho_j} f(x_j) \cdot W_{ij} \tag{5}$$

$$with \; W_{ij} = W(x_i - x_j, h)$$

Where $h$ is the smoothing length, $i$ and $j$ as particles, $m_i$ is the mass, $\rho_i$ is the density of the fluids, and $W_{ij} = W(x_i - x_j, h)$ is the weight function. The weight function should be constructed following several conditions such as positivity, compact, support, normalization, monotonically increasing and delta function behaviour [36-39].

Thus this can be directly translated to be the particle approximation shown in eqn. (6) for spatial derivative:

$$< \nabla \cdot f(x_i) >= -\sum_{j=1}^{N} \frac{j}{\rho_j} f(x_j) \cdot \nabla W_{ij} \tag{6}$$

where

$$\nabla W_{ij} = \frac{x_i - x_j}{r_{ij}} \frac{dW_{ij}}{dr_{ij}} = \frac{x_{ij}}{r_{ij}} \frac{dW_{ij}}{dr_{ij}} \tag{7}$$

Eqn. (6) indicates that the average values of the function at all particles in the support domain of particle $i$ are weighted by the gradient of the smoothing function. Eqn. (7) explains that the

gradient $\nabla W_{ij}$ is evaluated relative to particle *j*. The particle approximation allows the entire system to be represented by a finite number of particles that carry individual mass and space. Liu [30, 31] pointed out that this can be conveniently applied to hydrodynamics cases. The particle approximation introduces mass and density of the particle in the equation and approximation is done at every time step allowing the adaptive nature of the particles. Furthermore, the approximations are performed at all functions terms in Partial Differential Equations to produce a set of Ordinary Differential Equations thus allowing it to be solved using an explicit integration algorithm.

Another aspect relating to the use of SPH is the implementation of the smoothing function and the smoothing length, *h*. The smoothing function is used for both kernel and particle approximation to determine the interpolation pattern and the cut-off distance of the particle's sphere of influence. The smoothing function outlined in eqn. (8) was introduced by Monaghan and Lottanzio [40] became the most frequently [30] used smoothing function as it was found that it closely mimic a Gaussian function with a compact support even though the instability in the system remains. This function is called the cubic B-spline function. With *R* as the relative distance between the two points *x* and *x'*; $R = \frac{|x-x'|}{h}$.The smoothing function for a three-dimensional space can be written as:
with $W(x - x', h) = W(R, h)$

$$W(R,h) = \frac{3}{2\pi h^3} \times \begin{cases} \frac{2}{3} - R^2 + \frac{1}{2}R^3, & 0 \le R < 1, \\ \frac{1}{6}(2-R)^3, & 1 \le R < 2, \\ 0, & R \ge 2 \end{cases} \tag{8}$$

## 2.3 FLUID MECHANICS OF WATER IN ROAD SAFETY BARRIERS

The Navier-Stokes equation is the foundation to fluid mechanics as it has widely been considered to be the governing equation of motion for incompressible Newtonian fluid [41, 42]. Due to the Navier-Stokes equation being an unsteady, nonlinear, second-order partial differential equation, this makes the equation analytically unsolvable except for very simple flows [41]. Thus Computational Fluid Dynamics (CFD) is needed to solve the equation in this case.

To implement the Navier-Stokes in SPH, Liu [29, 30] substituted the SPH approximation for the function and its derivative in eqn. (5) and eqn. (6) to the Navier-Stokes equation, which leads to the set of commonly used SPH equations outlined in eqn. (9):

$$\begin{cases} \frac{D\rho_i}{Dt} = \sum_{j=1}^{N} m_j v_{ij}^{\beta} \frac{dW_{ij}}{dx_i^{\beta}} \\ \frac{Dv_i^{\alpha}}{Dt} = -\sum_{j=1}^{N} m_j \left( \frac{\sigma_i^{\alpha\beta}}{\rho_i^2} + \frac{\sigma_j^{\alpha\beta}}{\rho_j^2} \right) \frac{dW_{ij}}{dx_i^{\beta}} + F_i \\ \frac{De_i}{Dt} = \frac{1}{2} \sum_{j=1}^{N} m_j \left( \frac{p_i}{\rho_i^2} + \frac{p_j}{\rho_j^2} \right) v_{ij}^{\beta} \frac{\delta W_{ij}}{\delta x_i^{\beta}} + \frac{\mu_i}{2\rho_i} \varepsilon_i^{\alpha\beta} \varepsilon_i^{\alpha\beta} \end{cases} \tag{9}$$

Where $v_{ij} = v_i - v_j$ and $\alpha$ and $\beta$ superscripts represent the coordinate directions which the summation is taken (over repeated indices), ρ is the density, $v^{\alpha}$ is the velocity component, *e* is the internal energy, $\sigma^{\alpha\beta}$ is the total stress tensor and *F* is the external force i.e gravity. $\varepsilon$ is the shear strain rate of the viscous shear stress in Newtonian fluid with $\mu$ as the dynamic viscosity.

Thus the SPH method excels at modelling fluid boundaries over its grid based counterpart as it does not suffer from high distortions failure[17] that plagued FEA elements when modelling problems with large fluid motion. Additional problem that is solved with the use of SPH is the free surface interface between water and air elements in the model. The use of SPH eliminates the need to create a different set of elements to represent the air section of the barrier.

## 2.4 COUPLING OF SPH WITH FEA ELEMENTS

SPH suffers from the implementation of finite boundary conditions. The contact definition at the interface between the particles and finite element section must be defined accordingly [14, 43].

There are several methods that have been proposed for seamless interaction between the elements. Various contact algorithms can be found in literature for solid-fluid interfaces in numerical simulations. The contact relation of the surface between FEA elements and SPH particles elements have been modelled by either "master-slave"[44-46] relation or by the relative position of the boundary and the surface contact relation e.g "particle-to-particle" or "particle-to-surface" approach [47].

Alternative contact algorithm has also been explored by De Vuyst et al [48]. This alternative coupling method uses node-to-node contact rather than the previously mentioned algorithm. De Vuyst presented an algorithm that does not require the calculation of normal force to relate the frictionless sliding between discretised FEM bodies with particle bodies.

In coupling the analysis, special algorithm is available to be employed [47, 49-53]. These algorithm is needed to avoid un-natural penetration within the model[31]. Furthermore, the use of repulsive force [54, 55] or the Lennard-Jones penalty force can be applied [56] as viable options to treat the material interface in the model. Using SPH, Anghileri[17] was able to emulate the characteristics motion of water with higher precision than any other simulation method. The only drawback with SPH is the significant requirement of computer resources for the computation.

This research aims to attain the numerical coupling of SPH and FEM at high impact velocities. The LS-DYNA theoretical [57] manual suggests using the function nodes-to-surface contact type to couple the finite elements and SPH elements as the contact algorithm. This method was chosen in the research and achieved accurate coupling between meshless and meshed elements.

Although FEM is efficient at solving typical high speed problems, the high fluid motion created by materials with fluid properties such as water pose difficulties in elemental discretisation and contact modelling due to complexities as the problem size increases.

In PWFB, the distortion from the particles is high. This inadvertently leads to an increase of computational time. The setup for coupled analysis using FEA elements and SPH particles elements for numerical model at high speed impacts has not been deeply studied in road barriers, thus it is vital for the research to investigate the seamless transition between FEA elements and SPH particles at different sections of the barrier.

## 2.4 VALIDATION OF COUPLING TECHNIQUE

This study is to validate the numerical results using existing results available in the literature. Anghileri[17] tested several methods including the coupling of SPH and FEA elements to simulate the impact of a helicopter fuel tank with the ground. The numerical-experimental correlations that were obtained by Anghileri are used to validate the seamless interaction between the SPH and FEA elements.

A simplified model, as shown in Figure 1, of the fuel tank used by Anghileri was constructed with similar material properties and boundary conditions outlined in his paper. The model which has the dimension 750mm x 718mm x 300mm with an overall thickness of 2mm was constructed using solid modelling software. For purpose of model validation, similar outputs were obtained by tabulating the acceleration of nodes at the end point of the tank where it first hit the ground. The simulation results are plotted in Figure 2, which shows good agreement between the numerical results and the reference. However, slight discrepancies are evident between the two simulations due to differences in the model start point, output resolution, material properties and different model parameters. Nevertheless results were within the acceptable range.

This step of the study presents two significant points in the coupled analysis. Firstly, it can be inferred that the coupling is acceptable when impact is at low speeds (less than 12m/s). Secondly, since the model is constructed at full scale, it is plausible that full scale road barrier impact can be conducted later on in the research. Hence, this becomes a platform to continue coupled SPH and FEA elements for determining the energy absorption capacity of water.

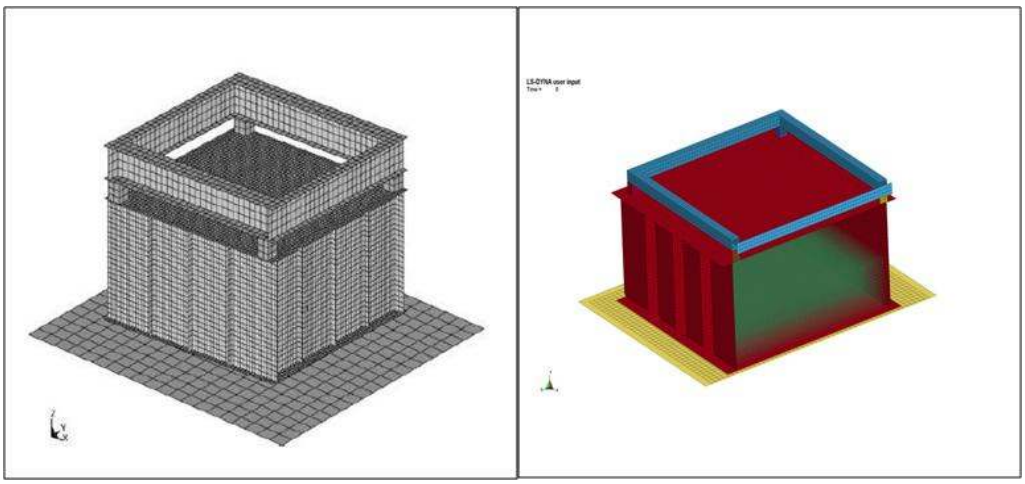

**Figure 1: Model of tank by Anghileri (left) and model of tank used in this study (right)**

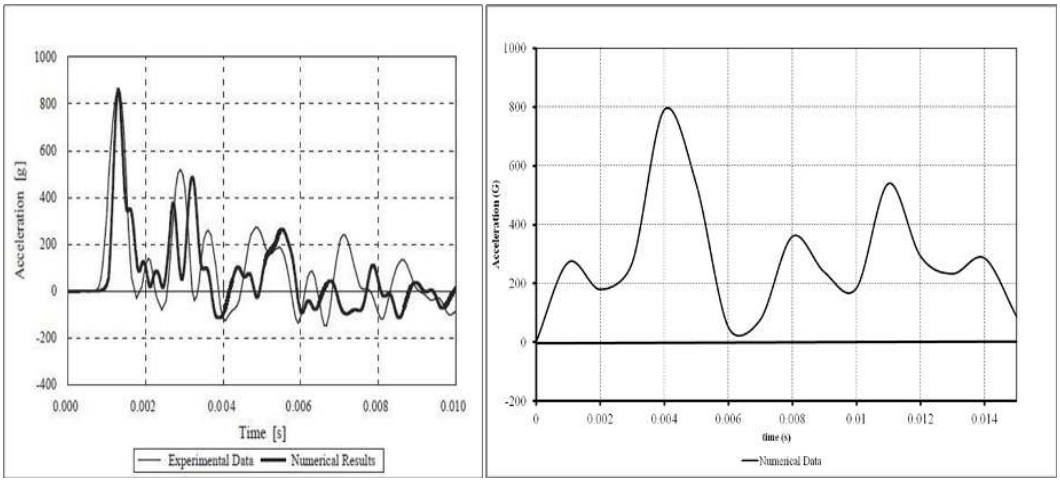


**Figure 2: Numerical-experimental correlation by Anghileri (left) in contrast to result obtained in this study (right)**

## 3. NUMERICAL MODEL

As shown in Figure 3, the preliminary road safety barrier impact model consists of 3 parts which are the shell container, impact block and particles that represent water. The rigid block will impact the shell container filled with water. Overall, the model uses approximately 300 shell elements, 1700 solid elements and 8000 particle elements.

The actual size of road barriers that the research worked on has the dimension 1200mm x 550mm x 375mm with a thickness of 12mm. In this study, the model is scaled 1:10 of the actual size of road safety barriers to ease computation requirement during simulation. The dimension of the scaled barrier model was set to be 120mm x 55mm x 37.5mm with 12mm thickness which reduced computation time in this preliminary study of coupled SPH and FEA. The impact height and location are assigned so that the impact is at the middle section of the rectangular shell container. The chosen impact location is intended to be at the weakest area of the barrier, which is horizontally located between 150mm to 550mm away from the end of the barrier. The height of the impact is placed to be the same height of the front bumper of a 2010 Toyota Yaris[58]. Translated to scale, the impact was 20mm from one end and 30mm from the bottom of the barrier. The model underwent reiterations with different water levels. The shell elements used to model the container are assumed to not break up or tear apart at any time during impact. This assumption is required so that the barrier or container remain fully enclosed to allow the water sloshing to

develop. Any breakage will lead to failure of the fluid in the barrier to slosh and absorb energy. The impact velocity was kept constant at 0.5m/s and the SPH elements were filled to different levels of 0%, 30%, 50%, 80% and 100% capacity. All simulations were carried out by parallel computing at the supercomputer facility in the university.

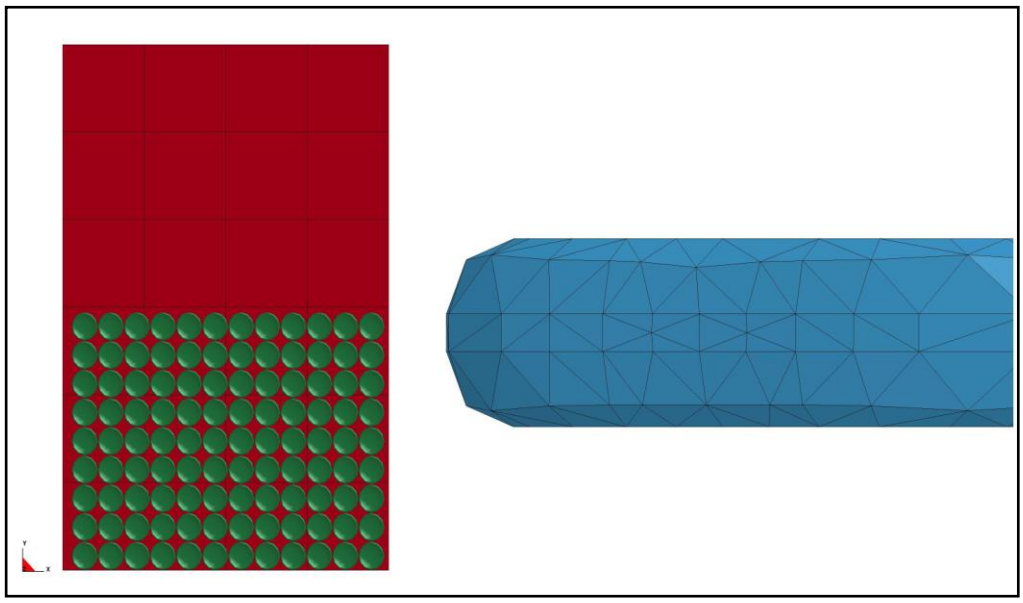

Figure 3: Impact System: Container with SPH water Particles Impacted by Block

### 3.1 FINITE ELEMENT MODEL OF SHELL CONTAINER

In water-filled barriers, fluid is filled into an enclosed container within the barrier. In this research the scaled model of the barrier, replicated by the container is initially filled to its capacity 0.00025m$^3$ (or 100%). The container is made up from High Density Polyethylene (HDPE) with piecewise linear plasticity and is modelled using shell elements. Since the study focuses on fluid structure interaction, rivets or bolt connections were ignored. The mesh of the container consisted of 288 four-node shell elements. As this study is interested in the energy absorption effect of water in road barriers, the ground interaction with the container was considered frictionless and the dimensions of the barrier are made constant. Further research will be done to examine the effect of these parameters to the overall energy absorption. It must also be assumed that the container will not break in any instances of the simulation. This assumption is done to allow sloshing by the water inside.

### 3.2 FINITE ELEMENT MODEL OF IMPACT BLOCK

A single block with solid elements was constructed to represent the impact vehicle. The front impact head is curved to mimic the front vehicle bumper that is expected to be the first part to impact a barrier [59, 60]. The material characteristics are those of rigid structural steel. The block approximately impacts the hollow container at 0.5m/sec at a 20 degree angle. The container is assumed to be in a stationary position prior to impact with block. The mesh of the impact block is made of 1677 solid elements. The block is considered rigid and its deformation after impact with the shell container was not investigated. Thus, the strain rate effects properties of the impact block are negligible.

### 3.3 MODEL OF WATER INSIDE THE CONTAINER

SPH was implemented to represent water inside the container. Enabling the (SPH) particles to represent water was carried out in steps. It was observed that the material for the water particles matched well with material NULL in LS DYNA. This was assigned as the material model for the water which was then assigned its density.

The couplings between FEA elements and SPH particles were explored in this research. The function “nodes_to_surface” contact type was assigned to couple the FEA and SPH elements. The

use of fluid formulation with normalization was utilised to smooth the interface between the coupled elements. The particles were distributed evenly across the shell container and at 100% filled capacity there are 8640 meshless particles inside the container. The cubic B-spline function shown in eqn. (8) is used as the SPH smoothing function.

The equation of state is another factor required in modelling the fluid. There are several models of the equations of state available in LS-DYNA [57]. This research used the Mie-Gruneisen Equation of State (EOS) outlined in eqn. (10) which defines pressure for compressed materials as:

$$p = \frac{\rho_0 C^2 \mu \left[1 + \left(1 - \frac{\gamma_0}{2}\right)\mu - \frac{\alpha}{2}\mu^2\right]}{\left[1 - (S_1 - 1)\mu - S_2 \frac{\mu^2}{\mu + 1} - S_3 \frac{\mu^3}{(\mu + 1)^2}\right]} + (\gamma_0 + \alpha\mu)E \qquad \textbf{(10)}$$

In Equation (10), μ is $\eta - 1$ where $\eta$ is the ratio of the densities before and after the disturbance, $\rho_0$ is the material density, $C$ is the bulk speed of sound, $\gamma_0$is the Gruneisen's gamma at the reference state, $\alpha$is the first order of correction to $\gamma_0$, $S_1$, $S_2$, $S_3$ are the coefficient slope in a linear Hugoniot line of the shock wave velocity slope and E is the internal energy per unit volume. The LS-Prepost platform in LS DYNA was used in this research where C, $S_1$, $S_2$, $S_3$, $\gamma_0$, $\alpha$ are user defined input parameters. In the initial setup of the simulations, the density was added in particle generation and C was set as the speed of sound in water which 1,484 m/s and all other parameters were left as zero [61].

Table 1: Material properties for all parts in impact model

| Material | Density (kg/m$^3$) | Poisson Ratio | Young's Modulus (GPa) | Yield Stress (MPa) |
|---|---|---|---|---|
| HDPE | 940.0 | 0.40 | 1.10 | 22.0 |
| Structural Steel | 7850.0 | 0.28 | 210.0 | 250.0 |
| Water | 1000.0 | - | - | - |

## 4. RESULTS AND DISCUSSION

The simulations underwent several iterations with different amounts of water. As the use of SPH method requires significant computational power, preliminary convergence verification was done to optimise the SPH particles and computer resources required in the simulation. The numerical model was executed using QUT's supercomputer facility. This study used up to 6 CPUs and each simulation took approximately 90 minutes.

The research aims to attain valuable insights in achieving seamless transition between FEA elements and SPH particles. The system stability in handling large motion of fluids at high speeds and the resulting sloshing of water are also of interest in this study. Furthermore, data from water in the vicinity of the container provided evidence of interaction between the water particles and the structural ements of the container.

The interface between the SPH particles with FE mesh indicated satisfactory coupling of the SPH and FEA. To check the stability of the system at high impact velocities, the velocity was increased to 10 m/s. It was observed that there were large penetrations at the interface of the FEA elements and SPH particles and caused some particles to burst out from the shell. In order to rectify such un-natural penetration and reinforce system stability, more user-defined constants were introduced into the EOS. This succeeded in preventing further penetration from occurring in the model. These additional user-defined constants however were obtained from literature [62, 63] and actual constants will need to be established from experimental studies for high speed impacts.

Figure 4 demonstrates the sequence impact responses of the water filled container and clearly shows the water particles moving within the enclosed container. The water is able to move arbitralily within the enclosed container in response to the impact by the block. Traditional FEA elements are unable to produce similar results due to the fact that gridded meshes do not allow elements to cross-over at high distortions. SPH succeeded in replicating the sloshing of water by

eliminating the need to create any elements for air within the enclosed container (which replicates the cavity of the barrier section). The sloshing interaction of the water after the impact of the container descibes the smooth connectivity between the elements

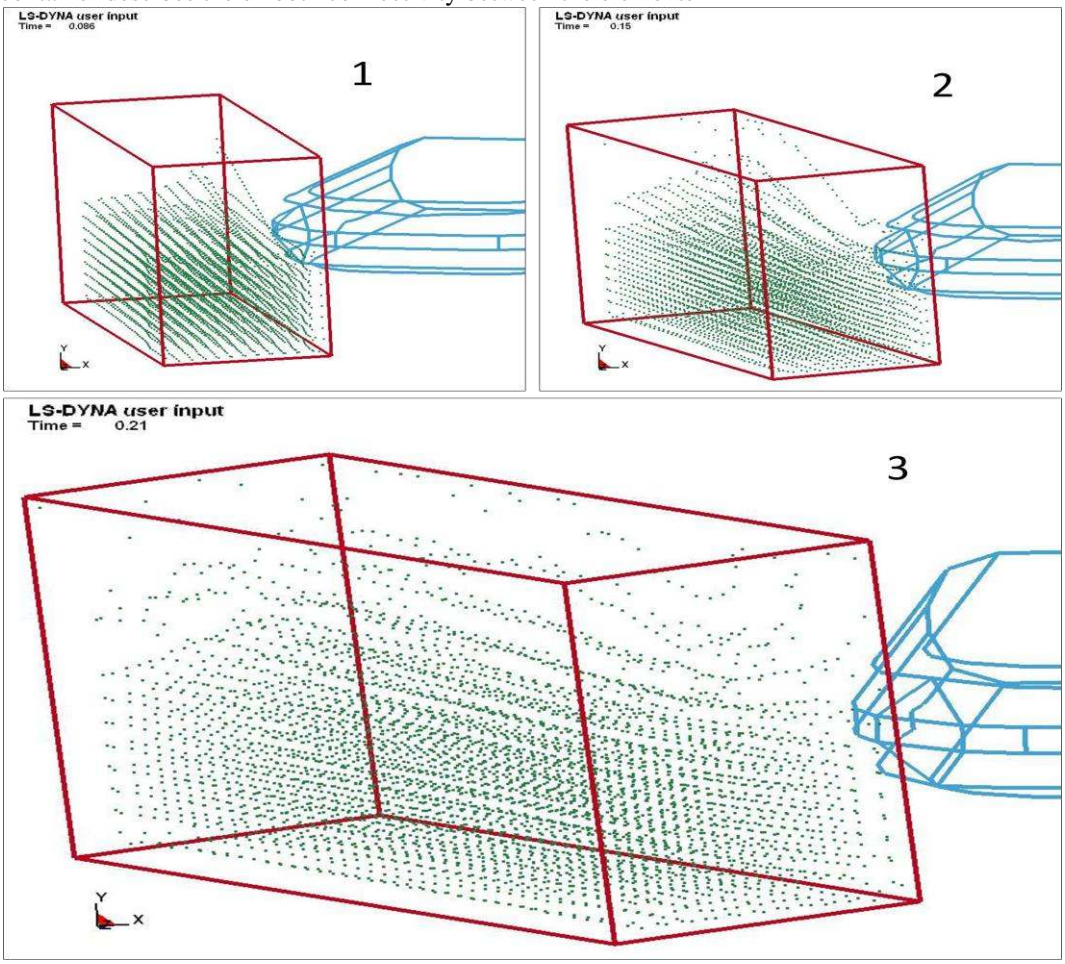


Figure 4: Clockwise sequence of FEA elements with SPH particles impacted by rigid block at 50% filled capacity

## 4.1 IMPACT RESPONSE AND ENERGY ABSORPTION OF CONTAINER

Investigations on the impact and energy absorption of the water filled container were carried out at different filled levels: 30%, 50%, 80% and 100% capacity. The impact of an empty container was also simulated for reference. Numerical models of all these cases were then impacted with a block at 0.5m/s initial velocity. Data from the simulations were obtained and tabulated. Figure 3 shows that the initial peak accelerations of the container seem to be independent of the fill level. This peak occurs around 0.03 second and shows that the inclusion of water does not alleviate the severity of this initial peak. The second peak in the acceleration however indicates that it depends on the fill level. This secondary peak at 0.04 seconds increases with fill level and is near zero for the empty case. The occurrence of an instantaneous secondary peak can be associated with the reaction forces that exist when water is present in the system.

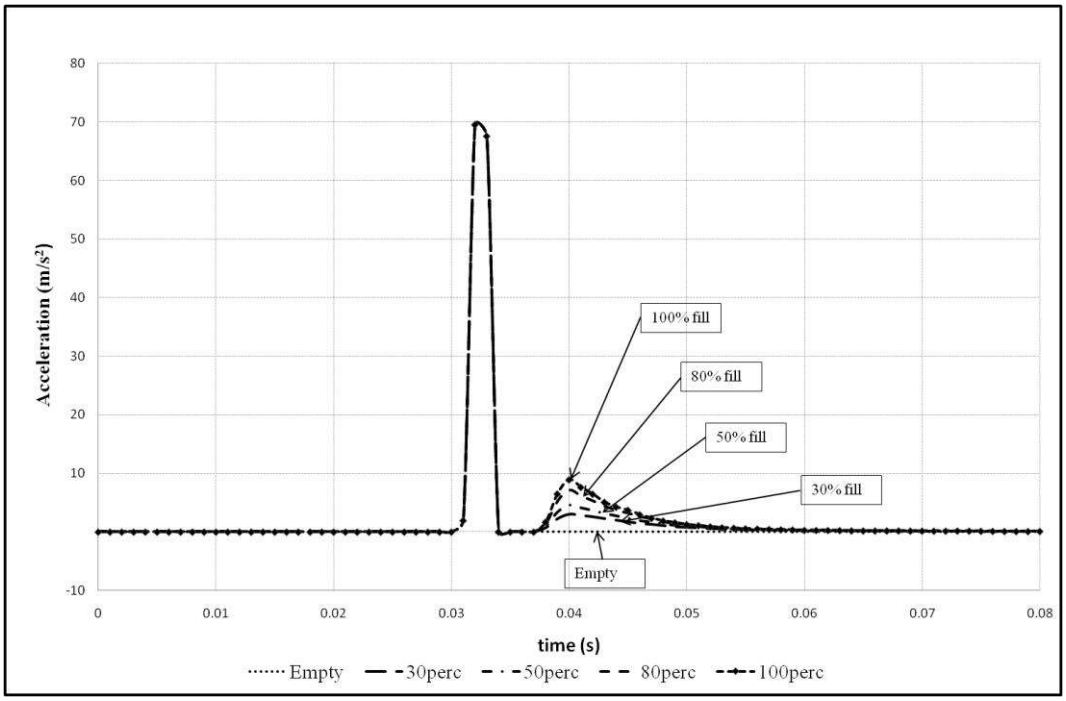


Figure 5: Resultant Acceleration of HDPE elements at Different Fill Levels

As observed in Figure 5, the secondary peaks that occur on all filled cases show that a force is exerted on the container (barrier) by the water inside. The height of the secondary peak for each fill level is related to the amount of water and indicates the force transfer between the SPH and the Finite Elements of the container at the interface. The peak of a 100% fill level is twice that of the peak at 50% fill level. These secondary peak accelerations which occur when there is fluid in the system are however small and less than or equal to 15% of the initial peak acceleration. The phenomenon of the secondary peaks needs further investigation to clarify how it benefits the deflection and energy absorption criteria of road safety barriers.

Figure 6 shows the kinetic energy absorbed by the container for different filled levels. It can be seen that without any water in the system, maximum (entire) kinetic energy is absorbed by the HDPE shell container. On the other hand, the minimum kinetic energy is absorbed by the container shell wall at 100% filled capacity. This suggests that the amount of kinetic energy absorbed by the container shell depends on the fill level. The initial peak in energy absorption (at 0.03sec) is same for all fill levels. The subsequent energy absorption response described by consecutive smooth reductions and peaks, is different for each fill level and indicates the absorption of energy by water. Furthermore, a container with less water undergoes higher energy spikes than their fuller counterparts.

Current simulation shows that water does not alleviate localised initial peak when the container was hit. However, the subsequent energy dissipation rate from the system correlates with the level of water in the container. Furthermore, due to the scale of the model and the low impact speeds, the existence of localised shocks that water experience after impact is indiscernible in the model. The concept of water shockwave due to the impact at higher speed requires more investigation. Steps must be taken to guarantee stability in simulation to study this phenomenon.

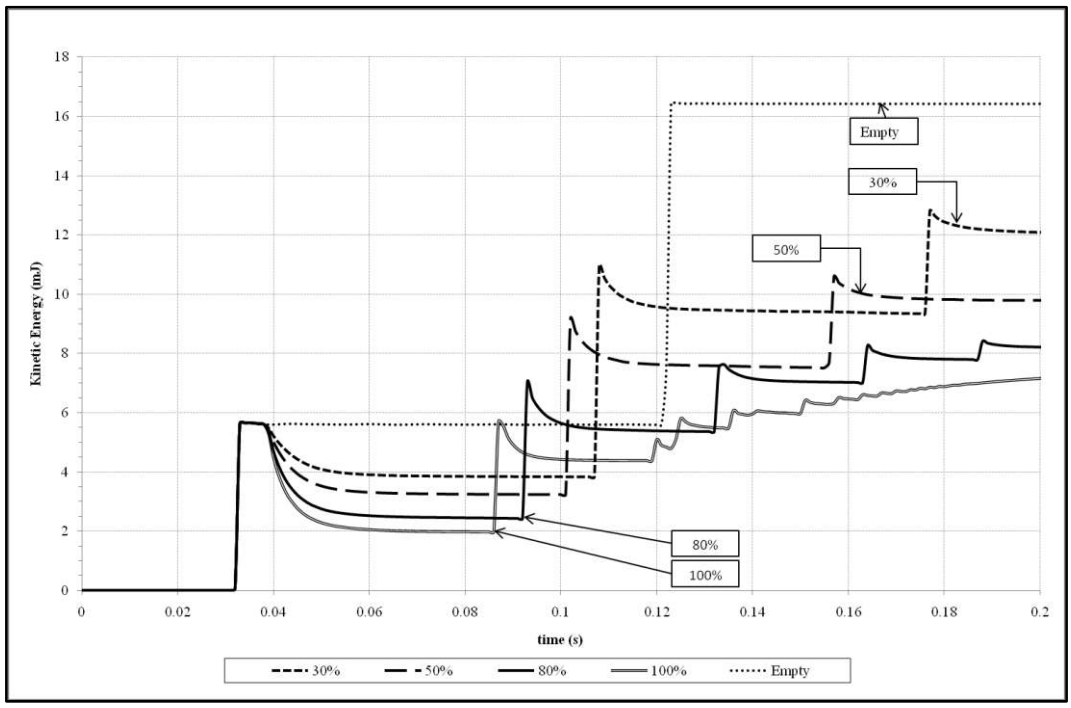


Figure 6: Kinetic Energy of Container at Different Fill Levels

## 4.2 ENERGY ABSORPTION OF WATER

Figure 7 illustrates the kinetic energy of the water for different fill levels, obtained as output from the simulations. As expected, the water at 100% fill has the most amount of energy post impact while the water at 30% fill level has the minimum amount of energy. The trend in the increase in the energy absorbed with increase in fill level confirms that the interface between the shell elements and water particles is functioning.

The results on the impact energy absorbed by the water were further analysed. Figure 8 shows the energy absorbed by the water with time for different fill levels. The amount of energy absorbed by the water at first increases with time, but soon remains sensibly constant over time. In order to use water effectively in PWFBs, the best compromise between energy absorption and fill level is needed. In the analyses carried out, the minimal energy absorption of water was 30% capacity with 20% energy absorbed from the overall energy of system. The increase of fill level from 30% to 50% enhanced the absorption capacity of water by 10%. At maximum fill level of 100%, water is able to absorb up to 45% of the total energy of the system. Thus, the energy absorption capacity of water in PWFBs can be determined for effective water usage in PWFBs. If more energy is absorbed by water, the demand on the container will be less and will reduce the likelihood of its failure. This shows that water does play an important role in absorbing impact energy. Although PWFBs with 100% fill level absorb the maximum amount of energy, the practicality of real world application of water in PWFB must be taken into consideration. The required barrier (wall) length, the logistics and transportation of water to the work zone are aspects to consider in the use of water filled barriers. Pumping the water in and out of the barriers have proven to be an issue for many PWFB applications [64]. Thus, it is imperative that the optimal water levels be determined for prudent water management in road safety barriers. Although water does absorb crash energy, the huge energy levels involved in roadside accidents may require the use of additional crash energy absorption materials in the barrier. The information presented in this paper will enable informed decisions to be made on the amount of water that can be practically used in a PWFB.

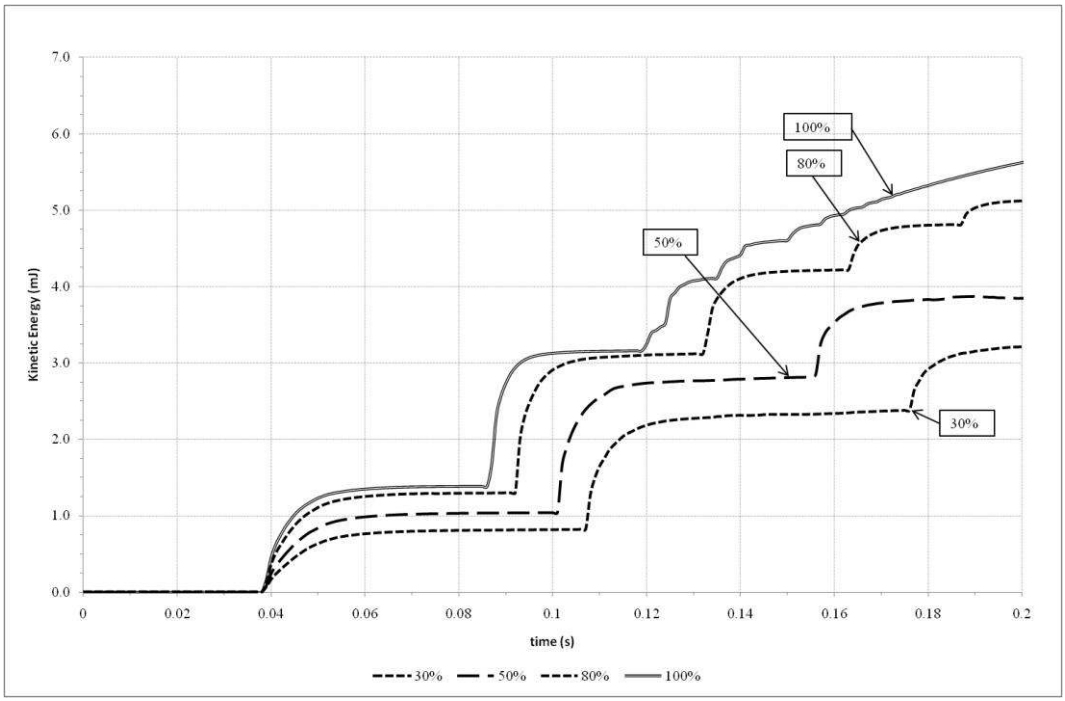


Figure 7: Kinetic Energy of Water at Different Fill Levels

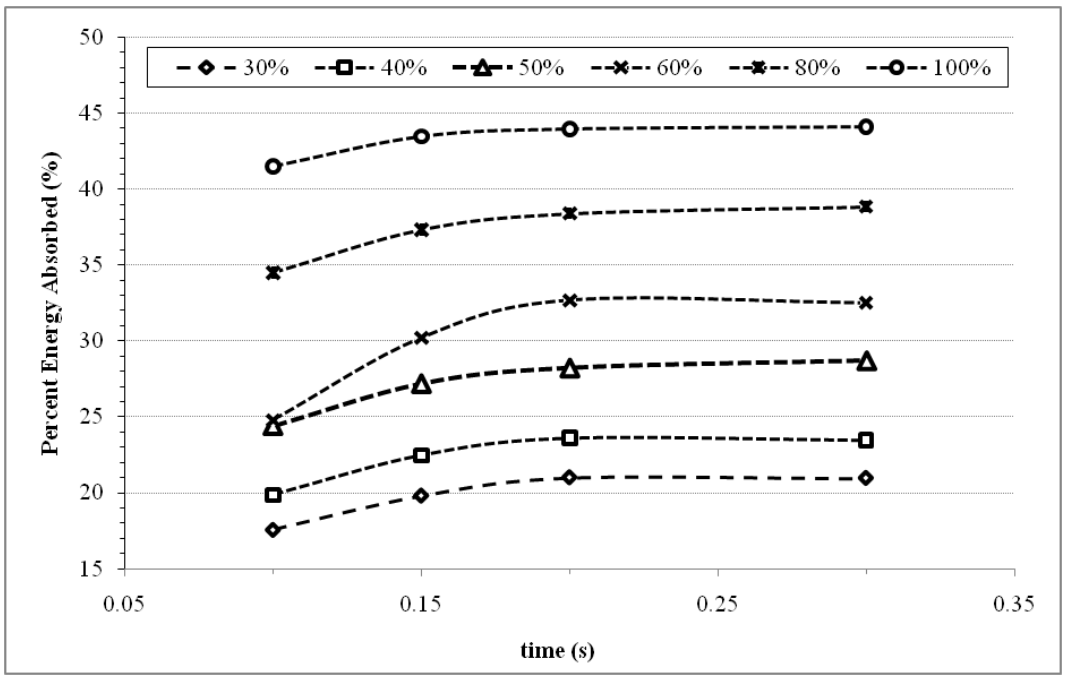


Figure 8: Percent Energy Absorbed at Different Time

## 5. CONCLUSION

Water has been used in PWFB only as deadweight to keep the barrier stationary, although its potential for energy absorption was known. The reaction of water inside PWFB in the event of a crash is important to better understand the post-impact behaviour and energy absorption of the water and the barrier. This paper presents the initial research carried out to simulate the impact response of a PWFB.

The aim of this study was to develop an effective fluid-structure interaction model based on the coupled SPH/FEM method which utilises the advantages of SPH and FEM. It was evident that the

motion of SPH particles captured, in the simulation, accurately mimics the fluidity of water when it comes into contact with the container. The water sloshing effects caused secondary peak accelerations of the container (barrier) as observed from the results of the simulations. It has been found that water plays an important role in absorption of impact energy of a PWFB. From the numerical simulations and results, the following conclusions can be drawn:

- The coupling of SPH and FEA is a powerful numerical modelling tool for impact simulations of PWFBs. The numerical results and observations in this research have proven the effectiveness of the developed fluid-structure interaction model based on the coupled FEA/SPH. Full scaled numerical modelling and impact experiments will be conducted for validation of this new model.
- Besides as deadweight, water in PWFB is also able to absorb some or even a major part of the impact energy. It can significantly reduce the failure possibility of barrier shell and therefore extend its' life-span. This finding is important for the future design of new generation of PWFBs.
- This research also highlighted some new findings pertaining to fill levels. The amount of water used in road safety barrier needs to be optimised. The results presented herein will enable informed decisions to be made regarding the practical use of water and its energy absorption capacity in a PWFB.

It should be mentioned here that this paper presented numerical results to determine the response and energy absorption of water in PWFB. The water levels were varied while other parameters such as the barrier dimensions and impact speed were left constant. These other parameters can be investigated in the future.

In continuation of the research, the next step is the creation of a full scale impact model. Furthermore, the fabrication of a new impact test rig is currently underway at QUT. Once completed, models from the ongoing research will be validated at the facility with actual experimental tests.

## 6. ACKNOWLEDGEMENT

This work is supported by an ARC Linkage Grant (ARC LP: 1020318). The support from Mr. Rory Gover through his useful discussions and suggestions and the contribution of the Industry Partner, Centurion Barrier Systems, are appreciated.

## 7. REFERENCES

1. Gudimetla, P., *New generation high energy absorbing barrier for improved road safety*. 2010.
2. Bureau of Infrastructure Transport and Regional Economics [BITRE], *Road deaths Australia - 2009 statistical summary*. 2010, Bureau of Infrastructure Transport and Regional Economics [BITRE],: Canberra
3. Sorock, G.S., T.A. Ranney, and M.R. Lehto, *Motor vehicle crashes in roadway construction workzones: An analysis using narrative text from insurance claims.* Accident Analysis & Prevention, 1996. **28**(1): p. 131-138.
4. Gover, R., Gu, Y.T., Thambiratnam, D.P, Gudimetla, P, *Impact characteristics of a flexible road barrier and vehicle crash response*. 2008, CRC Press (Taylor ans Francis Group).
5. Grzebieta, R.H., Zou, R., Jiang, T., Carey, A., *Roadside hazard and barrier crashworthiness issues confronting vehicle and barrier manufacturers and Government regulators.* 2008.
6. Borovins, M., Vesenjak,M., Ulbin, M., Ren, Z. *Simulation of crash tests for high containment levels of road safety barriers.* 2006.

7. Ulker, M.B.C., Rahman, M. S., Zhen, R., Mirmiran, A., *Traffic barriers under vehicular impact: from computer simulation to design guidelines.* Computer-Aided Civil and Infrastructure Engineering, 2008. **23**(6): p. 465-480.

8. Grzebieta, R., Cameron, J., Carey, A., Zou, R., *Water-filled plastic safety barrier systems.* Road and Transport Research, 2001. **10**(Compendex): p. 66-83.

9. Ren, Z. and M. Vesenjak, *Computational and experimental crash analysis of the road safety barrier.* Engineering Failure Analysis, 2005. **12**(6): p. 963-973.

10. Yuan, C. and J. Xianlong, *Dynamic response of flexible container during the impact with the ground.* International Journal of Impact Engineering, 2010. **37**(10): p. 999-1007.

11. Souli, M., A. Ouahsine, and L. Lewin, *ALE formulation for fluid-structure interaction problems.* Computer Methods in Applied Mechanics and Engineering, 2000. **190**(5-7): p. 659-675.

12. Wang, J. and M.S. Gadala, *Formulation and survey of ALE method in nonlinear solid mechanics.* Finite Elements in Analysis and Design, 1997. **24**(4): p. 253-269.

13. Gadala, M.S. and J. Wang, *ALE formulation and its application in solid mechanics.* Computer Methods in Applied Mechanics and Engineering, 1998. **167**(1-2): p. 33-55.

14. Tabri, K., Broekhuijsen, J., Matusiak, J., Varsta, P., *Analytical modelling of ship collision based on full-scale experiments.* Marine Structures, 2009. **22**(1): p. 42-61.

15. Sarrate, J., A. Huerta, and J. Donea, *Arbitrary Lagrangian-Eulerian formulation for fluid-rigid body interaction.* Computer Methods in Applied Mechanics and Engineering, 2001. **190**(24-25): p. 3171-3188.

16. Donea, J., S. Giuliani, and J.P. Halleux, *An arbitrary lagrangian-eulerian finite element method for transient dynamic fluid-structure interactions.* Computer Methods in Applied Mechanics and Engineering, 1982. **33**(1-3): p. 689-723.

17. Anghileri, M., L.-M.L. Castelletti, and M. Tirelli, *Fluid-structure interaction of water filled tanks during the impact with the ground.* International Journal of Impact Engineering, 2005. **31**(3): p. 235-254.

18. Toumi, M., M. Bouazara, and M.J. Richard, *Impact of liquid sloshing on the behaviour of vehicles carrying liquid cargo.* European Journal of Mechanics - A/Solids, 2009. **28**(5): p. 1026-1034.

19. Housner, G., *Dynamic pressures on accelerated fluid containers.* Bulletin of the Seismological Society of America, 1957. **47**(1): p. 15.

20. Babu, S.S. and S.K. Bhattacharyya, *Finite element analysis of fluid-structure interaction effect on liquid retaining structures due to sloshing.* Computers & Structures, 1996. **59**(6): p. 1165-1171.

21. Cho, J.R. and H.W. Lee, *Numerical study on liquid sloshing in baffled tank by nonlinear finite element method.* Computer Methods in Applied Mechanics and Engineering, 2004. **193**(23-26): p. 2581-2598.

22. Tabri, K., J. Matusiak, and P. Varsta, *Sloshing interaction in ship collisions--An experimental and numerical study.* Ocean Engineering, 2009. **36**(17-18): p. 1366-1376.

23. Godderidge, B., Turnock, S., Tan, M., Earl, C., *An investigation of multiphase CFD modelling of a lateral sloshing tank.* Computers & Fluids, 2009. **38**(2): p. 183-193.

24. Armenio, V. and M. La Rocca, *On the analysis of sloshing of water in rectangular containers: Numerical study and experimental validation.* Ocean Engineering, 1996. **23**(8): p. 705-739.

25. Delorme, L., A. Souto Iglesias, and S. Abril Pérez. *Sloshing loads simulation in LNG tankers with SPH*. 2005.

26. Ye, Z. and A. Birk, *Fluid pressures in partially liquid-filled horizontal cylindrical vessels undergoing impact acceleration.* Journal of pressure vessel technology, 1994. **116**: p. 449.

27. Faltinsen, O., Rognebakke, O., Lukovsky, I., Timokha, A., *Multidimensional modal analysis of nonlinear sloshing in a rectangular tank with finite water depth.* Journal of Fluid Mechanics, 2000. **407**: p. 201-234.

28. Anghileri, M., Castelletti, L., Francesconi, E., Milanese, A., Pittofrati, M., *Rigid body water impact-experimental tests and numerical simulations using the SPH method.* International Journal of Impact Engineering, 2011. **38**(4): p. 141-151.

29. Liu, G.R. and M.B. Liu, *Smoothed particle hydrodynamics : a meshfree particle method*. 2003, New Jersey: World Scientific. xx, 449 p.

30. Liu, M.B. and G.R. Liu, *Smoothed particle hydrodynamics (SPH): An overview and recent developments.* Archives of Computational Methods in Engineering, 2010. **17**(1): p. 25-76.

31. Liu, M.B., Liu, G. R., Lam, K. Y., Zong, Z., *Smoothed particle hydrodynamics for numerical simulation of underwater explosion.* Computational Mechanics, 2003. **30**(2): p. 106-118.

32. Swaddiwudhipong, S., M. Islamb, and Z. Liu, *High Velocity Penetration/Perforation Using Coupled Smooth Particle Hydrodynamics-Finite Element Method.* International Journal of Protective Structures, 2010. **1**(4): p. 489-506.

33. Lucy, L., *A numerical approach to the testing of the fission hypothesis.* The Astronomical Journal, 1977. **82**: p. 1013-1024.

34. Gingold, R.A. and J.J. Monaghan, *Smoothed particle hydrodynamics-theory and application to non-spherical stars.* Monthly Notices of the Royal Astronomical Society, 1977. **181**: p. 375-389.

35. Stellingwerf, R.F. and C.A. Wingate, *Impact Modelling with Smooth Particle Hydrodynamics.* Societa Astronomica Italiana, 1994.

36. Monaghan, J., *Smoothed particle hydrodynamics.* Reports on Progress in Physics, 2005. **68**: p. 1703.

37. Fulbright, M.S., W. Benz, and M.B. Davies, *A method of smoothed particle hydrodynamics using spheroidal kernels.* The Astrophysical Journal, 1995. **440**: p. 254-262.

38. Crespo, A., M. Gómez-Gesteira, and R.A. Dalrymple, *Modeling dam break behavior over a wet bed by a SPH technique.* Journal of Waterway, Port, Coastal, and Ocean Engineering, 2008. **134**: p. 313.

39. Gomez-Gesteira, M., *Using a three-dimensional smoothed particle hydrodynamics method for wave impact on a tall structure.* Journal of Waterway, Port, Coastal, and Ocean Engineering, 2004. **130**: p. 63.

40. Monaghan, J.J. and J.C. Lattanzio, *A refined particle method for astrophysical problems.* Astronomy and astrophysics, 1985. **149**: p. 135-143.

41. Cengel, Y.A. and J.M. Cimbala, *Fluid mechanics : fundamentals and applications*. McGraw-Hill series in mechanical engineering. 2006, Boston: McGraw-Hill Higher Education. xxv, 956.

42. Munson, B.R., Young, D.F., Okiishi, T.H., Huebsch, W.W., *Fundamentals of fluid mechanics*.5th Edition, 1998.

43. Gu, Y., *Meshfree methods and their comparisons.* International Journal of Computational Methods, 2005. **2**(4): p. 477-516.

44. Johnson, G.R., *Linking of Lagrangian particle methods to standard finite element methods for high velocity impact computations.* Nuclear Engineering and Design, 1994. **150**(2-3): p. 265-274.

45. Johnson, G.R. and S.R. Beissel, *Normalized smoothing functions for sph impact computations.* International Journal for Numerical Methods in Engineering, 1996. **39**(16): p. 2725-2741.

46. Sauer, M., *"Adaptive Kopplung des netzfreien SPH-Verfahrens mit finiten Elementen zur Berechnung von Impaktvorgaengen".* Adaptive Kopplung des netzfreien SPH-Verfahrens mit finiten Elementen zur Berechnung von Impaktvorgaengen, 2000.

47. Campbell, J., R. Vignjevic, and L. Libersky, *A contact algorithm for smoothed particle hydrodynamics.* Computer Methods in Applied Mechanics and Engineering, 2000. **184**(1): p. 49-65.

48. De Vuyst, T., R. Vignjevic, and J.C. Campbell, *Coupling between meshless and finite element methods.* International Journal of Impact Engineering, 2005. **31**(8): p. 1054-1064.

49. Chieragatti, R., Espinosa, C., Lacome, J.L., Limido, J., Mabru, C., Salaün, M., *Modelling high speed machining with the SPH method.* 2008.

50. Vignjevic, R., J. Campbell, and L. Libersky, *A treatment of zero-energy modes in the smoothed particle hydrodynamics method.* Computer Methods in Applied Mechanics and Engineering, 2000. **184**(1): p. 67-85.

51. Randles, P.W. and L.D. Libersky, *Smoothed Particle Hydrodynamics: Some recent improvements and applications.* Computer Methods in Applied Mechanics and Engineering, 1996. **139**(1-4): p. 375-408.

52. Gu, Y. and G. Liu, *Hybrid boundary point interpolation methods and their coupling with the element free Galerkin method.* Engineering Analysis with Boundary Elements, 2003. **27**(9): p. 905-917.

53. Gu, Y.T. and G.R. Liu, *A coupled element free Galerkin/boundary element method for stress analysis of two-dimensional solids.* Computer Methods in Applied Mechanics and Engineering, 2001. **190**(34): p. 4405-4419.

54. Monaghan, J.J., *SPH without a Tensile Instability.* Journal of Computational Physics, 2000. **159**(2): p. 290-311.

55. Vignjevic, R., T. de Vuyst, and J. Campbell, *The use of a homogeneous repulsive force for contact treatment in sph.* WCCM V, 2002.

56. Liu, M.B., Liu, G. R., Lam, K. Y., Zong, Z., *A new technique to treat material interfaces for smoothed particle hydrodynamics.* Computational Mechanics - New Frontiers for New Millennium, 2001: p. 977-982.

57. Hallquist, J., *LS-DYNA3D theoretical manual.* Livermore software technology corporation, 1998, 2006.

58. National Crash Analysis Center and G.W. University. *Finite element model archive*. 2010 06/09/2010 [cited 2010 08/26]; Available from: http://www.ncac.gwu.edu/.

59. Council, T.R.B.N.R., *NCHRP Report 350: Recommended Procedures for the Safety Performance Evaluation of Highway Features*. 1993.

60. Seo, J., D.G. Linzell, and Z. Rado, *Computational and experimental modification of portable sign structure design following NCHRP 350 criteria.* International Journal of Crashworthiness, 2011. **16**(2): p. 111-116.

61. Kennedy, J., Kennedy,James, Shah, Qasim H., Chen, Shen-Yeh, Thiyahuddin, M. I et al., *SPH interface with FE meshed elements* in *SPH interface with FE meshed elements* Yahoo, Editor. 2000.

62. Liu, M.B., G.R. Liu, and K.Y. Lam, *Investigations into water mitigation using a meshless particle method.* Shock Waves, 2002. **12**(3): p. 181-195.

63. Davis, R.O., *Further comments on thermodynamic response of Mie-Gruneisen materials.* Zeitschrift für Physik B Condensed Matter, 1973. **17**(1): p. 63-70.

64. Lohse, C., S. Velinsky, and D. Bennett, *Temporary barrier usage in work zone*. 2007, UC Davis: Davis